Journal of Statistical Mechanics: Theory and Experiment
An IOP and SISSA journal

# Realistic dispersion kernels applied to cohabitation reaction–dispersion equations

**Neus Isern, Joaquim Fort and Joaquim Pérez-Losada**

Departament de Física, Universitat de Girona, 17071 Girona, Catalonia, Spain
E-mail: neus.isern@udg.edu, joaquim.fort@udg.edu and joaquim.perez@udg.edu

Received 21 May 2008
Accepted 23 September 2008
Published 15 October 2008

Online at stacks.iop.org/JSTAT/2008/P10012
doi:10.1088/1742-5468/2008/10/P10012

**Abstract.** We develop front spreading models for several jump distance probability distributions (dispersion kernels). We derive expressions for a cohabitation model (cohabitation of parents and children) and a non-cohabitation model, and apply them to the Neolithic using data from real human populations. The speeds that we obtain are consistent with observations of the Neolithic transition. The correction due to the cohabitation effect is up to 38%.

**Keywords:** dynamics (theory), population dynamics (theory)

J. Stat. Mech. (2008) P10012



1742-5468/08/P10012+17$30.00

## Contents



## 1. Introduction

In systems where dispersion and reaction processes coexist, front spreading may be observed. A front can be defined as a moving profile connecting an initial, unstable state with a final, stable state. For example, in population dynamics the final state corresponds to the maximum population density that can be supported by the environment, whereas in combustion flames it corresponds to the burned state.

Previous work on front spreading includes analytical calculation of front speeds for (i) reaction terms such that linear analysis is appropriate (pulled fronts), as well as for the non-linear case (pushed fronts) [1], (ii) sequential reaction and dispersion [2], (iii) dispersal kernel effects leading to the breakdown of classical diffusion [3], (iv) biased random walks [4, 5], (v) age-structured systems [6, 7], (vi) distributed delays [8, 9], etc. (For a recent review see [10].)

Front propagation models have been extensively applied to study physical and biological systems including population dispersals [5], combustion flames [11], Taylor–Couette and Rayleigh–Bénard experiments [1], viral infections [12], tumor growth [13], etc.

In most studies on human population dynamics, the velocity of fronts has been calculated with Fisher's equation ($c_{\mathrm{Fisher}} = \sqrt{2aD}$, where $a$ is the initial growth rate



J. Stat. Mech. (2008) P10012

and $D$ the diffusion coefficient) or, more recently, with the HRD (hyperbolic reaction–diffusion) equation [14, 15]. In the HRD model, it is assumed that (i) each individual (or particle) rests for a time interval $T$ between successive jumps, and (ii) the duration of jumps is negligible compared to the rest time $T$. This leads to the front speed (for the detailed derivation, see [14])

$$c_{\mathrm{HRD}} = \frac{2\sqrt{aD}}{1 + (aT/2)}. \tag{1}$$

Fisher's speed ($c_{\mathrm{Fisher}} = \sqrt{2aD}$) is recovered for $T \ll 1/a$, so it is valid only if the rest time $T$ is negligible.

Fisher's and HRD equations include the dispersion just as a parameter, namely the diffusion coefficient ($D = \langle \Delta^2 \rangle / 4T$, where $\langle \Delta^2 \rangle$ is the mean squared displacement of jumps). In this work, we study the effect of using the whole dispersion kernel (distribution of the dispersal probability on jump distance $\Delta$) on front speeds. We tackle this problem not only from hypothetical distributions, but also using data from real human populations in order to obtain more realistic results and compare them to the observed front speed of the Neolithic transition in Europe.

Results depending on the full kernel have to be obtained from an integrodifferential evolution equation for the population density, rather than a differential equation [14]. In previous work, we have already used integrodifferential evolution equations for population dynamics models in order to study persistency effects on front speeds [7], fronts from biased random walks [4] and fronts for interacting species [16]. However, realistic dispersion distributions obtained from observed human populations have not been applied before. In section 2 we present two possible evolution equations (a cohabitation model and a non-cohabitation one). Then we obtain analytical and numerical results for the front speed for both evolution equations. In section 3 we consider several-distance dispersion kernels in 2D, while in section 4 we apply Laplace and Gauss 2D kernels. These results are applied to the Neolithic transition in Europe in section 5 using real dispersion data from six human populations. In section 6 we describe a stochastic model which we compare with the deterministic results. Finally, in section 7 we present our conclusions.

## 2. Evolution equations

In order to study the effect of the dispersion kernel on front speeds, we need an integrodifferential evolution equation for the population density $p(x, y, t)$. A possible expression for the evolution equation is [4, 7, 16]

$$p(x, y, t + T) = \int_{-\infty}^{+\infty} \int_{-\infty}^{+\infty} p(x + \Delta_x, y + \Delta_y, t) \phi(\Delta_x, \Delta_y) \, \mathrm{d}\Delta_x \, \mathrm{d}\Delta_y + R_T \left[ p(x, y, t) \right] - p(x, y, t). \tag{2}$$

The first term in equation (2) is the dispersal term, where the probability $\phi(\Delta_x, \Delta_y)$ is the dispersion kernel, and gives the probability per unit area that an individual initially placed at $(x + \Delta_x, y + \Delta_y)$ moves to $(x, y)$ during a time interval $T$ of one generation [14].



J. Stat. Mech. (2008) P10012

$R_T[p(x,y,t)]$ in equation (2) is the solution of the logistic growth equation, widely used in population dynamics [17],

$$R_T\left[p(x,y,t)\right] = \frac{p(x,y,t)\; p_{\max} \mathrm{e}^{aT}}{p_{\max} + p(x,y,t)\left(\mathrm{e}^{aT}-1\right)}, \tag{3}$$

where $p_{\max}$ is the carrying capacity. Equation (3) gives the final population density, due to population growth, after a time interval $T$ from the initial value $p(x,y,t)$. So, the last two terms in equation (2), $R_T[p(x,y,t)] - p(x,y,t)$, correspond to the net growth (natality–mortality balance) during $T$.

However, according to equation (2), after a generation new individuals appear due to reproduction at $(x,y)$ while parents have moved to $(x-\Delta_x, y-\Delta_y)$, i.e., parents leave their children behind when the former migrate. But this is not realistic for human populations; thus we use a more realistic evolution equation [4, 7, 16]:

$$p(x,y,t+T) = R_T\left[\int_{-\infty}^{+\infty}\int_{-\infty}^{+\infty} p(x+\Delta_x, y+\Delta_y, t)\phi(\Delta_x,\Delta_y)\,\mathrm{d}\Delta_x\,\mathrm{d}\Delta_y\right]. \tag{4}$$

The difference between equation (2) and equation (4) is a very important point. It is thus shown in figure 1 for the 1D case and a population at a single position at $t = 0$ (figure 1(a)). For equation (4), figure 1(b), the initial population migrates (full columns) and the population growth (hatched columns) takes place at the destination position. On the other hand, for equation (2), figure 1(c), population growth (hatched column) takes place only at the initial position $x$ due to the whole initial population, while part of this initial population has already migrated (full columns). So, from now on, equation (2) and its results will be named as non-cohabitation (NCohab), since parents migrate leaving their children behind, and equation (4) and its results will be named as cohabitation (Cohab).

## 3. Several-distance dispersion model

For real populations, the migrated distances per generation are usually continually distributed. But available data are recorded in intervals, so here we consider a discrete approximation with a kernel that allows dispersion to multiple discrete distances. Therefore, assuming an isotropic kernel, the linear distribution of probability can be expressed as a sum of Dirac deltas[1]

$$\varphi\left(\Delta\right) = 2\pi\Delta\phi\left(\Delta\right) = \sum_{i=0}^{n} p_i \delta(\Delta - r_i), \tag{5}$$

where $p_i$ is the probability for the individuals to move a distance $r_i = i \cdot d$, for $i = 0, 1, 2, \ldots, n$, with $d$ the width of the intervals used when recording the data.

Below we search for the front speed using analytical methods (CSRW, DSRW) and numerical simulations.

[1] The linear distribution of probability, $\varphi(\Delta)$, is the integration over the azimuthal coordinate $\theta$ of the 2D kernel, $\phi(\Delta)$. For an isotropic kernel, i.e., independent of $\theta$, the relation between the two distributions is $\varphi(\Delta) = 2\pi\Delta\phi(\Delta)$.



J. Stat. Mech. (2008) P10012

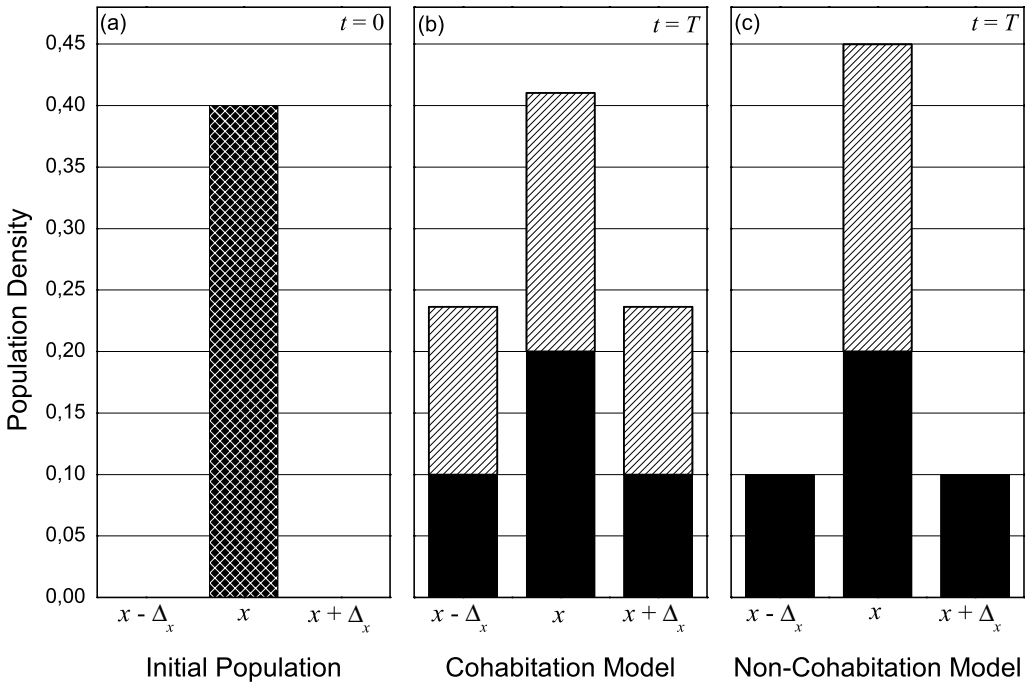


**Figure 1.** Comparison of cohabitation (equation (4)) and non-cohabitation (equation (2)) models in 1D. Initially the population is at a single position $p(x, t = 0)$ (a). In (b) and (c) full columns correspond to the dispersed population (parents) and hatched columns to the population growth (children). ($p_0 = 0.5$, $\phi(\Delta_x) = \delta(x \pm \Delta_x)$, $a = 0.028$ yr$^{-1}$, $T = 32$ yr.)

### 3.1. Continuous-space random walks (CSRW)

In order to find an analytical expression for the front speed, we apply some simplifications to the evolution equation. Firstly, as the population density at the leading edge of the front is low, equation (3) can be linearized there, becoming

$$R_T\,[p(x, y, t)] = p(x, y, t)\,\mathrm{e}^{aT}. \tag{6}$$

Moreover, since we have assumed an isotropic kernel, the front is azimuthally symmetric, so it can be considered approximately planar for $t \to \infty$ and $r \to \infty$. Then, choosing the $x$-axis as parallel to the local velocity of the front, $c \equiv |c_x|$, we look for constant-shape solutions with the form $p = \bar{p}\exp[-\lambda(x - ct)]$. Applying these simplifications to cohabitation equation (4), it may be rewritten as

$$\mathrm{e}^{\lambda cT} = \mathrm{e}^{aT} \int_{-\infty}^{+\infty} \int_{-\infty}^{+\infty} \mathrm{e}^{-\lambda\Delta_x}\phi(\Delta_x, \Delta_y)\,\mathrm{d}\Delta_x\,\mathrm{d}\Delta_y. \tag{7}$$

Finally, changing the coordinate system to polar coordinates, i.e., defining $\Delta \equiv \sqrt{\Delta_x^2 + \Delta_y^2}$ and $\theta \equiv \tan^{-1}(\Delta_y/\Delta_x)$, and using equation (5), we find an expression for the front velocity[2],

$$c_{\mathrm{Cohab}} = \min_{\lambda>0} \frac{\ln\left[\mathrm{e}^{aT}\sum_{i=0}^{n} p_i I_o(\lambda i d)\right]}{\lambda T}, \tag{8}$$

[2] The value of $d$ for CSRW is related to the mean squared displacement by $\langle\Delta^2\rangle = \sum_{i=0}^{n} p_i (id)^2$.



J. Stat. Mech. (2008) P10012

where $I_0(\lambda id)$ is the modified Bessel function of the first kind and order zero,

$$I_0\left(\lambda id\right) = \frac{1}{2\pi}\int_0^{2\pi} \exp\left(\lambda id\cos\theta\right)\,\mathrm{d}\theta. \tag{9}$$

Applying the same steps to the non-cohabitation equation (2), we obtain the expression for the front velocity (see footnote 2),

$$c_{\mathrm{NCohab}} = \min_{\lambda>0} \frac{\ln\left[\left(\mathrm{e}^{aT}-1\right)+\sum_{i=0}^{n} p_i I_o(\lambda id)\right]}{\lambda T}. \tag{10}$$

### 3.2. Reactive random walk simulations

Random walk numerical simulations follow the evolution of the population density in space and time. We consider a 2D grid of $3000 \times 3000$ nodes, with the initial condition $p(x=0, y=0, t=0)=1$, and $p(x, y, t=0)=0$ at every other node $(x, y)$. The evolution of the population is computed by repeating the following steps at each time interval ($T=1$ generation):

(i) We apply the dispersion kernel (5), but as the grid is Cartesian, the density is in fact distributed into the four edges of $n$ squares of side $2r_i = 2id$.[3] Thus, to each of the $8i$ nodes of the $i$-square corresponds a fraction $(p_i/8i)$ from the initial population.

(ii) The final population at each node is computed applying the population growth equation (3) to the result of step (i) (in the case of equation (4)) or applying equation (3) to the initial population and adding the result to that of step (i) (in the case of equation (2)).

### 3.3. Discrete-space random walks (DSRW)

In the CSRW approach (section 3.1) we consider a continuous space. But the simulation grid (section 3.2) is necessarily discrete, and this in fact modifies the kernel shape. Thus, the results from these two methods may be different. Therefore, here we suppose a discrete space in order to reproduce analytically the results obtained from the numerical simulations.

We first discretize equation (4) so that the kernel is square shaped as in the simulations. The dispersion term, namely

$$\int_{-\infty}^{+\infty}\int_{-\infty}^{+\infty} p(x+\Delta_x, y+\Delta_y, t)\phi(\Delta_x, \Delta_y)\,\mathrm{d}\Delta_x\mathrm{d}\Delta_y, \tag{11}$$

as a result of the discretization, becomes

$$p_0\,p(x,y,t) + \sum_{i=1}^{n}\frac{p_i}{8i}\Bigg\{\sum_{j=-i}^{i}\left[p(x+r_i, y+r_j, t)+p(x-r_i, y+r_j, t)\right] + \sum_{j=-i+1}^{i-1}\left[p(x+r_j, y+r_i, t)+p(x+r_j, y-r_i, t)\right]\Bigg\}. \tag{12}$$

[3] The value of $d$ for DSRW (and numerical simulations) is related to the mean squared displacement by the approximation $\langle\Delta^2\rangle = \sum_{i=0}^{n}(p_i/8i)\sum_{j=-i}^{i-1} 4[(id)^2+(jd)^2]$.



J. Stat. Mech. (2008) P10012

Applying now the same simplifications as for the CSRW (section 3.1) we obtain that the expression for the front speed is (see footnote 3)

$$c_{\mathrm{Cohab}} = \min_{\lambda>0} \frac{\ln\left[\mathrm{e}^{aT}\ \Psi(\lambda d)\right]}{\lambda T}, \tag{13}$$

where

$$\Psi(\lambda d) \equiv p_0 + \sum_{i=1}^{n} \frac{p_i}{4i}\left[1 + \sum_{j=1}^{i-1} 2\cosh(\lambda j d) + (2i+1)\cosh(\lambda i d)\right]. \tag{14}$$

Following the same method as above we find that the speed expression for the non-cohabitation equation (2) is (see footnote 3)

$$c_{\mathrm{NCohab}} = \min_{\lambda>0} \frac{\ln\left[\left(\mathrm{e}^{aT}-1\right) + \Psi(\lambda d)\right]}{\lambda T}. \tag{15}$$

## 4. Continuous dispersion models

In this section, instead of a multiple Dirac delta for the kernel (section 3), we consider isotropic continuous probability distributions in 2D.

In order to find analytical results we apply the same simplifications as in section 3: linearization of the growth equation and assumption of constant-shape front solutions $p = \bar{p}\exp[-\lambda(x-ct)]$. In this way, using again polar coordinates as in the CSRW, we obtain the following general expression for the cohabitation equation (4):

$$c_{\mathrm{Cohab}} = \min_{\lambda>0} \frac{\ln\left[\mathrm{e}^{aT}\int_0^{+\infty}\varphi(\Delta)\, I_0(\lambda\Delta)\ \mathrm{d}\Delta\right]}{\lambda T}, \tag{16}$$

where, as in equation (5), $\varphi(\Delta) = 2\pi\Delta\phi(\Delta)$ (see footnote 1).

The exact solution for this expression can be obtained from the value of $\lambda$ that satisfies $\mathrm{d}c_{\mathrm{Cohab}}/\mathrm{d}\lambda = 0$. Thus $\lambda$ is to be calculated from the relation

$$\tilde{\varphi}(\lambda)\ln\left[\mathrm{e}^{aT}\tilde{\varphi}(\lambda)\right] = \lambda\tilde{\varphi}'(\lambda), \tag{17}$$

where we have defined $\tilde{\varphi}(\lambda) \equiv \int_0^{+\infty}\varphi(\Delta)I_0(\lambda\Delta)\mathrm{d}\Delta$ and $\tilde{\varphi}'(\lambda) \equiv \mathrm{d}\tilde{\varphi}(\lambda)/\mathrm{d}\lambda$.

Applying the same steps to the non-cohabitation equation (2), we obtain the expression

$$\beta + \tilde{\varphi}(\lambda)\ln\left[\beta + \tilde{\varphi}(\lambda)\right] = \lambda\tilde{\varphi}'(\lambda), \tag{18}$$

where we have introduced $\beta \equiv \mathrm{e}^{aT} - 1$.

Some important kernels that have been widely applied to population dispersal are the Gauss and Laplace distributions [18]–[20]. These two kernels will also allow us to derive explicit equations for the front speed. In contrast to the case for previous work in 1D [3, 20, 21], here we consider a 2D space, as is necessary for application to the Neolithic transition (section 5).



J. Stat. Mech. (2008) P10012

### 4.1. Gauss distribution

The Gauss linear probability distribution is $\varphi(\Delta) = (2\Delta/\alpha^2)\mathrm{e}^{-(\Delta/\alpha)^2}$, so we obtain that

$$\tilde{\varphi}\,(\lambda) = \mathrm{e}^{\alpha^2\lambda^2/4}. \tag{19}$$

For the cohabitation equation (4), using equation (19) in equation (17) we obtain the exact result,

$$c_{\mathrm{Cohab}} = \alpha\sqrt{\frac{a}{T}}. \tag{20}$$

For the non-cohabitation equation (2), an exact solution cannot be found, but expanding equation (18) up to second order in $\alpha\lambda$ ($\alpha\lambda \ll 1$), we obtain the following explicit result:

$$c_{\mathrm{NCohab}} = \frac{\alpha}{2T}\sqrt{\frac{1+\beta\ln(1+\beta)}{(1+\beta)\ln(1+\beta)}} \times \ln\left[(1+\beta)^{(1+\beta)/[1+\beta\ln(1+\beta)]} + \beta\right]. \tag{21}$$

### 4.2. Laplace distribution

The Laplace linear probability distribution can be expressed as $\varphi(\Delta) = (\Delta/\alpha^2)\mathrm{e}^{-\Delta/\alpha}$, so we have that

$$\tilde{\varphi}\,(\lambda) = 1/(1-\alpha^2\lambda^2)^{3/2}. \tag{22}$$

The second-order approximation in $\alpha\lambda$ ($\alpha\lambda \ll 1$) for the front speed for the cohabitation equation, i.e., when using equation (22) in equation (17), is

$$c_{\mathrm{Cohab}} = \frac{\alpha}{T}\sqrt{1+\frac{3}{2aT}}\left(aT + \frac{3}{2}\ln\left[1+\frac{2aT}{3}\right]\right). \tag{23}$$

For the non-cohabitation equation, the second-order expansion in $\alpha\lambda$ ($\alpha\lambda \ll 1$) for equation (18) leads to the expression

$$c_{\mathrm{NCohab}} = \frac{\alpha}{T}\sqrt{\frac{(3/2)+(1+(5/2)\beta)\ln(1+\beta)}{(1+\beta)\ln(1+\beta)}} \times \ln\left[\left(\frac{1+((2/3)+(5/3)\beta)\ln(1+\beta)}{(1+\beta)\ln(1+\beta)}\right)^{3/2} + \beta\right]. \tag{24}$$

## 5. Application to the Neolithic transition

We apply the results from sections 3 and 4 to the Neolithic transition, i.e., the transition from hunter–gatherer to agricultural economics (the corresponding front speed has been measured from archaeological data on the first arrival of farmer populations [30]). We study two cases: (i) a simple approximation with single-distance dispersion (migration to nearest neighbors), and (ii) a more realistic case using mobility data from real populations (using both discrete and continuous kernels).



J. Stat. Mech. (2008) P10012

**Table 1.** Front speeds for the simplified model. The front speeds have been computed for the six human populations with the cohabitation equation (4) and the non-cohabitation one (2), using the values of the parameters $\langle\Delta^2\rangle$ and $p_0$ from the present table, and the extreme values of the range $a = 0.028 \pm 0.005$ yr$^{-1}$ ($v_{\min}$ and $v_{\max}$).

| | Population | $\langle\Delta^2\rangle$ (km$^2$) | $p_0$ | $v_{\min\ \mathrm{Cohab}}$ (km yr$^{-1}$) | $v_{\max\ \mathrm{Cohab}}$ (km yr$^{-1}$) | $v_{\min\ \mathrm{NCohab}}$ (km yr$^{-1}$) | $v_{\max\ \mathrm{NCohab}}$ (km yr$^{-1}$) |
|---|---|---|---|---|---|---|---|
| A | Gilishi15 [26] | 1003 | 0.54 | 0.850 | 1.010 | 0.659 | 0.734 |
| B | Gilishi25 [26] | 1210 | 0.40 | 0.899 | 1.055 | 0.693 | 0.764 |
| C | Shiri15 [26] | 2197 | 0.19 | 1.161 | 1.335 | 0.891 | 0.967 |
| D | Yanomamo [27] | 1728 | 0.19 | 0.926 | 1.066 | 0.711 | 0.772 |
| E | Issocongos [28] | 404 | 0.41 | 0.521 | 0.612 | 0.402 | 0.443 |
| F | Parma [28] | 508 | 0.77 | 0.674 | 0.825 | 0.533 | 0.611 |

The generation time that we apply in all cases is $T = 32$ yr, which was estimated in reference [9] as the mean age of the parents when a child is born (not necessarily the first one).

The range of values for the initial growth rate $a$ that we use at the rest of the paper has been estimated from data for four human populations (Pitcairn [22], Bass Strait [22] and Tristan da Cunha [23] Islands, and the United States population during the nineteenth century [24]). Fits to exponential growth of the population data from the three islands yield $a = 0.029\,95 \pm 0.001\,19$ yr$^{-1}$ for Pitcairn, $a = 0.026\,26 \pm 0.000\,52$ yr$^{-1}$ for Bass Strait and $a = 0.025\,27 \pm 0.000\,32$ yr$^{-1}$ for Tristan da Cunha. The growth rate calculated from the same logistic equation as was used by Lotka [24] for the US is $a = 0.031\,35 \pm 0.000\,63$ yr$^{-1}$. These four values yield the range $a = 0.028 \pm 0.005$ yr$^{-1}$ (80% confidence level). For populations colonizing a new habitat prior to the existence of the modern health and medicine [25], we are not aware of any population number time series leading to higher values of $a$.

### 5.1. Simplified model

Here we analyze a simplified model in which individuals can either stay at the initial position, with a persistency (probability of resting) $p_0$, or migrate to a single distance $d$, determined by the values of persistency $p_0$ and the mean squared displacement (mobility) $\langle\Delta^2\rangle$ (see footnotes 2 and 3).

In table 1 we present the parameter values and computed speeds for four preindustrial farmer populations (Gilishi15 [26], Gilishi25 [26], Shiri15 [26] and Issocongos [28]), the Yanomamo [27] (who are horticulturists), and the modern populations in the Parma Valley [28] already considered by Ammerman and Cavalli-Sforza [29]. The values for the front speed have been calculated for both the cohabitation equation (4) and the non-cohabitation one (2), using the CSRW (section 3.1) and the minimum and maximum values of the range $a = 0.028 \pm 0.005$ yr$^{-1}$, obtained above.

In figure 2 we present results for both evolution equations (2) and (4), obtained with the three methods (CSRW, DSRW and simulations), the mean mobility value of populations A, B and C ($\langle\Delta^2\rangle = 1531$ km$^2$), and two values of the persistency: (i) an



J. Stat. Mech. (2008) P10012

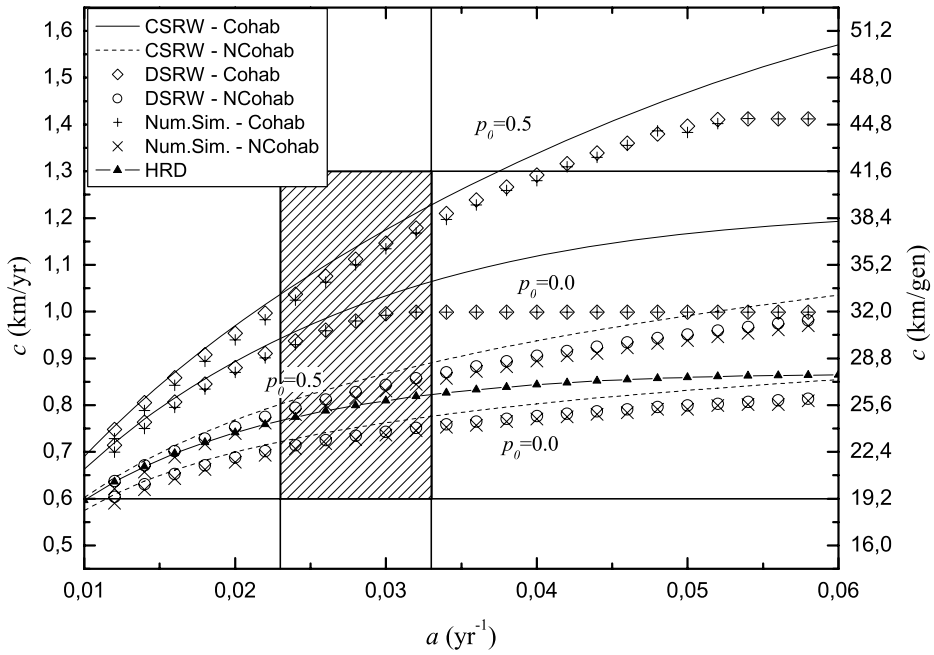


**Figure 2.** Front speeds for single-distance dispersion kernels. The speeds for the cohabitation equation (4), the non-cohabitation equation (2) and the HRD equation (1), have been computed using the mobility value $\langle\Delta^2\rangle = 1531$ km$^2$ and persistencies $p_0 = 0.0$ and 0.5. The hatched area corresponds to the observed ranges for $a$ and $c$.

extreme case with all individuals migrating, $p_0 = 0.0$, and (ii) a more realistic value, $p_0 = 0.5$ [7]. Front speed values in figure 2 have been computed over a large range of $a$, and note that in all cases the speed increases and tends to a maximum for large values of $a$ (discrete methods saturate at this speed) which corresponds precisely to $d$ km/gen. We can understand this limit intuitively as follows. Since this is a single-distance dispersion model, $d$ is the distance individuals move along the $x$ direction when they migrate, and thus, $d$ km/gen must be the maximum possible speed[4].

From figure 2 it can be seen that the speeds from the non-cohabitation equation (2) are always lower than those from the cohabitation equation (4); up to 34% lower when comparing results from the CSRW (full and dashed curves in figure 2). This was to be expected because according to equation (2) just the parent generation can disperse, whereas using equation (4) it is the whole population that can migrate (parents and children); see figure 1.

Comparing the results from the two values of the persistency in figure 2, we find that the front speed increases with the persistency, as could be expected[5] for populations with

[4] The value of $d$ is calculated differently for the CSRW case (see footnote 2) and the DSRW case and simulations (see footnote 3). Thus the speed limits obtained are different for continuous-space and discrete-space random walks (figure 2).

[5] Front speed increases with persistency because the jump distance $d$ has been calculated from the same value of the diffusion coefficient $D = \langle\Delta^2\rangle/4T$; so a larger probability of staying implies that those who migrate have to move a larger distance $d$ (see footnotes 2 and 3). Therefore, the front speed increases. This effect cannot be predicted by equation (1) (full line and triangles in figure 2), for example, as it only depends on $D$.



J. Stat. Mech. (2008) P10012

the same mobility value. We can also see this effect on table 1, where populations E and F have similar mobilities but population F has a higher persistency and thus a higher front speed. On the other hand, in table 1 we can also observe how for populations with the same persistency (C and D) a higher mobility (and thus, a higher diffusion coefficient $D = \langle \Delta^2 \rangle / 4T$) yields a higher speed.

The 95%-confidence-level speed for the Neolithic transition in Europe is currently estimated as 0.6–1.3 km yr$^{-1}$ [30]. In figure 2, the hatched box delimits this range for the initial growth rate range obtained above (0.023–0.033 yr$^{-1}$). Thus, although we obtain different speed values for each model, they all lie within the observed range for the speed of the Neolithic transition. However, from table 1, we see that whereas for the cohabitation equation (4) the calculated speeds are consistent with the observed range, for populations with low mobilities (E and F) the non-cohabitation equation (2) yields lower front speeds than the observed range for the Neolithic transition (up to 33% lower for population E).

### 5.2. Several-distance Dirac deltas model

Now we use the dispersion kernels obtained from real dispersion data for the six populations studied above. Firstly, we consider the dispersion kernels for three of these populations (namely, A, B and C in table 1),

$$\begin{aligned} P_{\mathrm{A}} &= \{0.54; 0.17; 0.04; 0.25\}, \\ P_{\mathrm{B}} &= \{0.40; 0.17; 0.17; 0.26\}, \\ P_{\mathrm{C}} &= \{0.19; 0.07; 0.22; 0.52\}, \end{aligned} \tag{25}$$

where the values correspond to the probabilities $p_i$ for distances $\{2.4; 14.5; 36.2; 60.4\}$ km.[6] For the sake of clarity, in figure 3 we show the results only for these three populations (computed with the results from sections 3.1 and 3.3). Here it is seen that the speeds obtained using the full kernel are consistent with the observed range (hatched area), and that again results from equation (2) are lower than those from equation (4) (22%–28% lower), for the same reasons as were given in the previous subsection.

In table 2 we present the front speed values computed with the cohabitation and non-cohabitation models (using the CSRW) for all six populations and the range $a = 0.028 \pm 0.005$ yr$^{-1}$ obtained above. The dispersion kernels used for populations D, E and F are

$$P_{\mathrm{D}} = \{0.19; 0.54; 0.17; 0.04; 0.04; 0.02\} \tag{26}$$

for distances $\{5.0; 30.0; 50.0; 70.0; 90.0; 110.0\}$ km,

$$P_{\mathrm{E}} = \{0.42; 0.23; 0.18; 0.08; 0.07; 0.02; 0.01; 0.01\} \tag{27}$$

for distances $\{2.3; 7.3; 15; 25; 35; 45; 55; 100\}$ km and

$$P_{\mathrm{F}} = \{0.77; 0.04; 0.04; 0.03; 0.03; 0.01; 0.01; 0.02; 0.05\} \tag{28}$$

for distances $\{1.3; 4.5; 9.5; 16.5; 25.5; 36.5; 49.5; 64.4; 81.5\}$ km.

[6] These values are the means for each interval from Stauder's data [26] according to the calculation of mobility by Ammerman and Cavalli-Sforza [29]. The distances correspond to $d = 2.4$ km and $i = \{1; 6; 15; 25\}$ in the kernel expression (5).



J. Stat. Mech. (2008) P10012

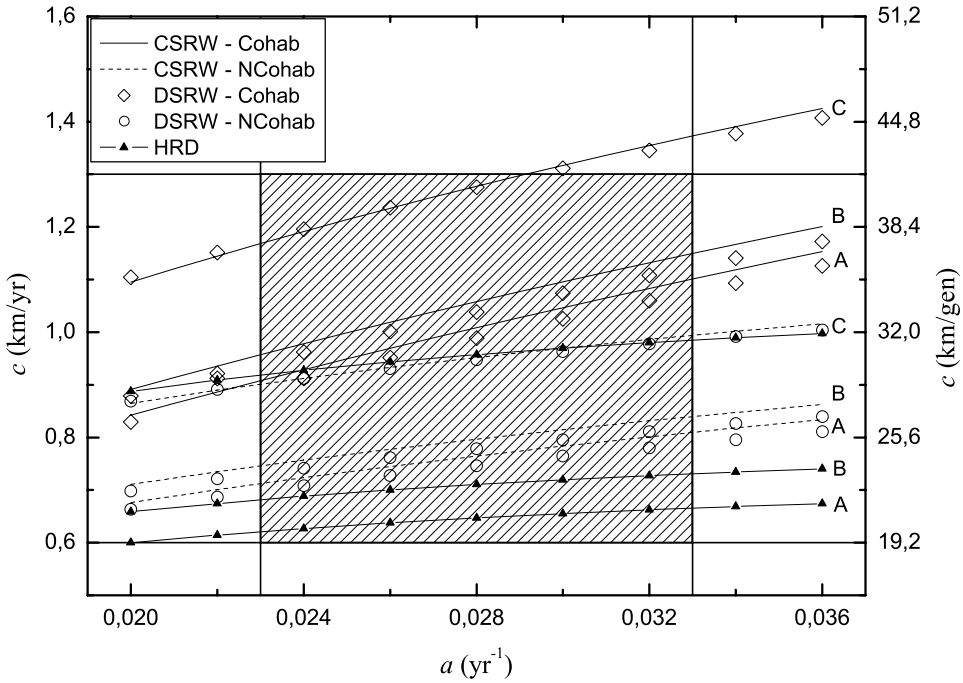


**Figure 3.** Front speeds for three real human dispersal kernels. The speeds for the cohabitation equation (4) and the non-cohabitation equation (2) are computed using kernel (25) (results for each population are labeled). The results for equation (1) are calculated from the value of $D$ for each population obtained from kernels (25) (see table 1). The hatched area corresponds to the observed ranges for $a$ and $c$.

**Table 2.** Front speeds for the Dirac deltas model. The front speeds have been computed for the six human populations with the cohabitation equation (4) and the non-cohabitation one (2), using the dispersion kernels from the text (section 5.2) and the extreme values of the range $a = 0.028 \pm 0.005$ yr$^{-1}$ ($v_{\min}$ and $v_{\max}$).

| | Population | $v_{\min\ \mathrm{Cohab}}$ (km yr$^{-1}$) | $v_{\max\ \mathrm{Cohab}}$ (km yr$^{-1}$) | $v_{\min\ \mathrm{NCohab}}$ (km yr$^{-1}$) | $v_{\max\ \mathrm{NCohab}}$ (km yr$^{-1}$) |
|---|---|---|---|---|---|
| A | Gilishi15 [26] | 0.908 | 1.101 | 0.712 | 0.810 |
| B | Gilishi25 [26] | 0.957 | 1.150 | 0.746 | 0.840 |
| C | Shiri15 [26] | 1.196 | 1.397 | 0.920 | 1.011 |
| D | Yanomamo [27] | 1.179 | 1.435 | 0.927 | 1.062 |
| E | Issocongos [28] | 0.737 | 0.940 | 0.608 | 0.737 |
| F | Parma [28] | 0.800 | 1.008 | 0.651 | 0.774 |

Comparing results from tables 1 and 2 we see that, in all cases, the front speed is faster when using the full kernel. The jump distance $d$ used in the previous section will always be lower than the longer possible distance of the kernel, and when individuals have a certain probability of moving further, the front speed increases. Thus, the correction introduced by using the full kernel will be more important for those populations with a certain



J. Stat. Mech. (2008) P10012

probability of migrating to distances much higher than the value of $d$ calculated from $\langle\Delta^2\rangle$. For example, for populations D and E, the corrections introduced by applying the full kernel are of approximately 30% and 48% respectively for the cohabitation equation (34% and 59% for the non-cohabitation equation). For both populations, individuals can move to large distances (110 and 100 km respectively), while for the simplified model the dispersion distance $d$ is about 41 km for population D and about 26 km for population E (see footnote 2).

On the other hand, we can see that the values of the front speed for population C in tables 1 and 2 are approximately the same. This can be explained mathematically because for these populations, the characteristic dispersal distance for the simplified model, $d \simeq 51$ km (see footnote 2), is similar to the maximum dispersed distance, 60 km. But it can also be explained qualitatively from the dispersion kernel (25), as for this population over 50% of individuals move to a single, long-range distance. Thus, this kernel behaves approximately as if the whole population could either not move or migrate just to a single distance (as in the simplified model studied in the previous section). This is also why in figure 3 there is a good agreement between the results from the non-cohabitation equation (2) and the HRD equation (1) for population C (figure 2 shows that equation (1) is a good approximation to the non-cohabitation model in this case[7]), while for A and B the difference is up to 20%.

Here we have shown that, if a population has a strong long-range dispersal component, then (i) its predicted speeds are faster, and (ii) the HRD equation (1) is a good approximation to the exact non-cohabitation model (2).

Referring to the speed values obtained, except for populations C and D for equation (4) and large values of the growth rate $a$, they are all within the range of observed speed for the Neolithic transition (0.6–1.3 km yr$^{-1}$ [30]). But even the speeds for populations C and D are marginally consistent with the observed range. Therefore, we conclude that the application of realistic human kernels to reaction–dispersion equations yields front speeds which are consistent with the values obtained from archaeological data. It is important to note that the whole kernel is necessary, because the single-distance model yielded speeds slower than the observed range for populations E and F (table 1).

### 5.3. Several-distance continuous model

Now we apply Laplace and Gauss probability distributions. For the sake of brevity, we consider the populations A, B and C from previous subsections. We calculate the value of the parameter $\alpha$ for both distributions from the mobility $\langle\Delta^2\rangle$ of each population ($\alpha^2 = \langle\Delta^2\rangle$ for the 2D Gauss distribution, and $\alpha^2 = \langle\Delta^2\rangle/6$ for the 2D Laplace distribution).

Comparing the results obtained from the Gauss and Laplace distributions, in figure 4 we can see that the speed for Laplace distribution is always faster. This is due to the fact that, for the same value of $\langle\Delta^2\rangle$, the Laplace distribution has higher values of probability at large distances than the Gauss distribution.

In figure 4 we also see that, whereas the difference between speeds from the Laplace distribution and kernel (25) for populations A and B is lower than 12%, for population C

[7] HRD equation (1) was deduced [14] from an equation analogous to equation (2), and thus it is an approximation to it.



J. Stat. Mech. (2008) P10012

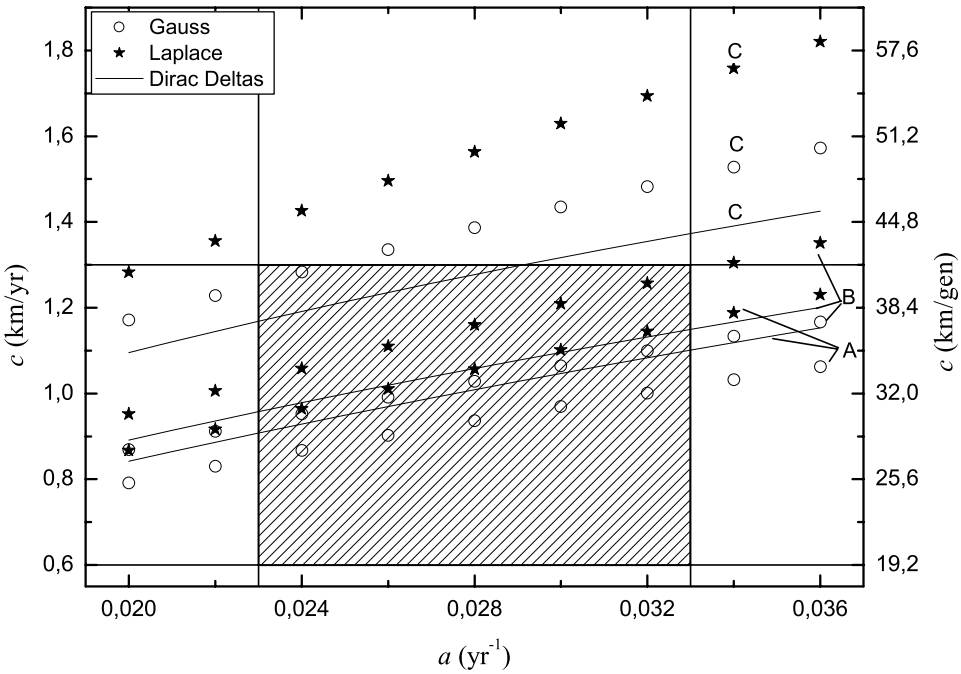


**Figure 4.** Front speeds from continuous probability distributions. Speeds obtained from the Gauss and Laplace cohabitation equations (20) and (23), using the mobility values for each population obtained from kernels (25) (see table 1). Dirac deltas correspond to the speeds from CSRW and the cohabitation equation in figure 3. The hatched area corresponds to the observed ranges for $a$ and $c$.

results from the Laplace distribution are about 30% faster. For the Gauss distribution, we see that the difference from the speeds obtained with the Dirac deltas kernel (25) is also larger for population C. This is due to the fact that for population C the distribution maximum is displaced to larger distances than for the other two populations and thus, there is a larger probability tail for population[8] C.

Here we have shown that, in the absence of a long-range dispersal component, discrete and continuous kernels lead to similar speeds (figure 4, populations A and B). However, long-range dispersal can make continuous kernels grossly overestimate the front speed (figure 4, population C).

## 6. Stochastic model

In the previous sections, all the results for the front speed have been obtained from deterministic models. Even the numerical simulations correspond to the deterministic equations, and differ from the results for the CSRW (section 3.1) due to the discretization of space.

However, population dynamics is a stochastic process that could introduce corrections to the deterministic front propagation [31]. In this section we describe a stochastic model

[8] For population C, the tail probability for distances beyond the range considered in equation (25) is about 40% (twice higher than for populations A and B).



J. Stat. Mech. (2008) P10012

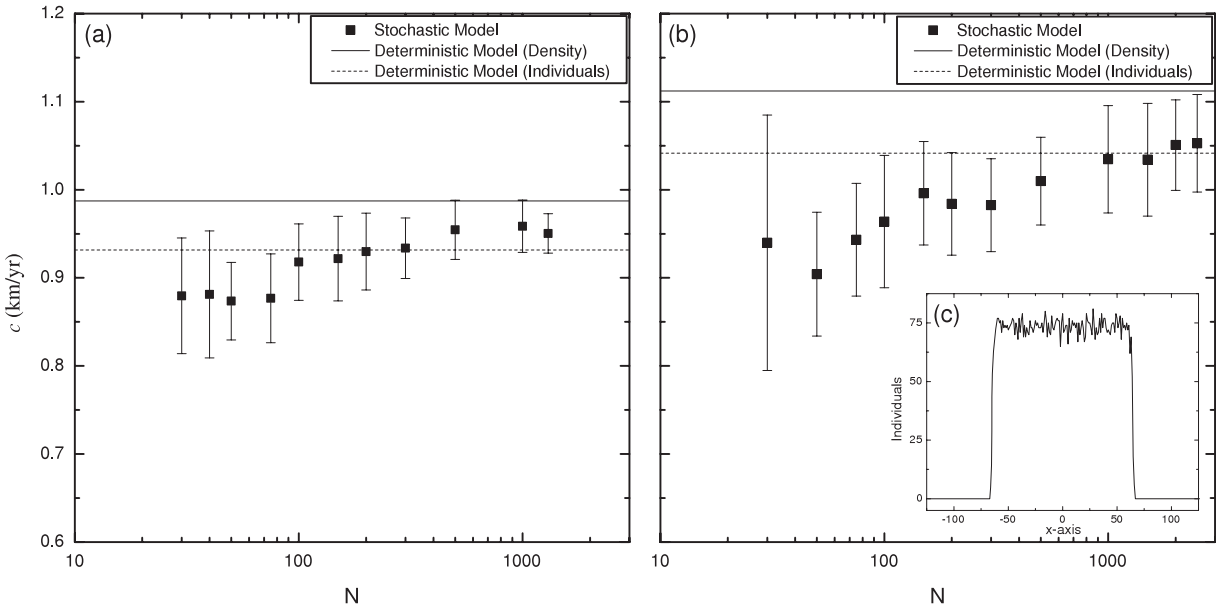


**Figure 5.** Front speeds for the stochastic model. Front speeds for (a) $p_0 = 0.0$ and (b) $p_0 = 0.5$ are represented for different values of $N$ (maximum number of individuals per cell), and compared with the deterministic model (solid and dashed lines). (c) shows a front profile for $N = 75$ individuals ($a = 0.028$ yr$^{-1}$).

that we apply to the simplified model studied in section 5.1. We perform the numerical simulations repeating the following steps for each time interval ($T$):

(i) For the dispersion process, we first assign *to each individual* a random value $n$ in the interval $[0, 1)$, so if $n < p_0$ the individual stays, and otherwise it migrates. Here, as in the simplified model (section 5.1) individuals can only migrate to the eight nearest neighbors on a square with equal probability. So each individual who can migrate is assigned randomly an integer value between 0 and 7 (each corresponding to one of the eight possible final positions). Finally, the position of each individual is changed according to this random value.

(ii) The reaction process is computed as in section 3.2, but since here we are dealing with individuals (instead of population densities) the final value is converted to an integer (by simply truncating the computed number).

In figure 5 we show the stochastic results obtained for different values of the number of individuals per cell $N$ (and $a = 0.028$ yr$^{-1}$). The error bars give the standard deviation of 16 simulations. In order to compare the results from the stochastic model with the deterministic simulations, we have used that the value of the carrying capacity for the Neolithic is $p_{\max} = 1.28$ hab km$^{-2}$ following reference [32]. This value of $p_{\max}$ corresponds to $N = 1306$ individuals per cell when $d = 31.95$ km ($p_0 = 0.0$) (see footnote 3), or to $N = 2613$ individuals per cell when $d = 45.19$ km ($p_0 = 0.5$) (see footnote 3). When the number of individuals per cell reaches the carrying capacity for the Neolithic the results for front speed from the stochastic model are very close to the deterministic ones (full horizontal lines in figure 5); they are about 3% slower than the deterministic speed when $p_0 = 0.0$ and about 5% slower when $p_0 = 0.5$. Nevertheless, this difference is

due not only to the randomness of the process, but also to the effect of using a discrete number of individuals (instead of a continuous population density). As shown in the figure, when performing simulations with the deterministic model but with a discrete number of individuals (dashed horizontal lines) the front speed obtained is slower than when using population densities; and we see that for large $N$ the results from the stochastic model lie between the results from the two deterministic simulations.

## 7. Concluding remarks

In this paper we have developed discrete and continuous models for reaction–dispersion systems with dispersion kernels. We have applied these models to the Neolithic transition using dispersion data sets from real human populations. Other authors [8, 33] have previously studied the Neolithic transition using data from real populations assuming that each individual is either a non-disperser or a disperser, with the same distance for all dispersers. However, here we have used full kernel expressions and, for the first time, we have applied them to a cohabitation evolution equation, equation (4).

This cohabitation equation, equation (4), is more realistic for human populations since they do not leave their children behind when migrating as happens with equation (2) (figure 1). Since equation (4) implies that more population migrates per generation time, the front speeds are faster than those from equation (2). For real populations, this difference is very important: up to 38% faster for the populations studied (table 2). However, the front speeds are still consistent with the observed range for the Neolithic transition (0.6–1.3 km $\mathrm{yr}^{-1}$ [30]). In the simplified model ignoring the kernel shape (table 1) this is no longer true for some populations (E and F). Thus, the whole kernel is essential when modeling human dispersals.

We also have provided new explicit equations for the front speed for the Gauss and Laplace 2D distributions and the cohabitation model (4) (section 4).

## Acknowledgments

Funded by the European Commission (grant NEST-28192-FEPRE), the MEC-FEDER (grant FIS-2006-12296-C02-02) and the Generalitat de Catalunya (grant SGR-2005-00087). NI was supported by the MEC under the FPU program.

## References

[1] van Saarloos W, 2003 *Phys. Rep.* **386** 29
[2] Fort J, 2007 *J. Appl. Phys.* **101** 094701
[3] Méndez V, Pujol T and Fort J, 2002 *Phys. Rev.* E **65** 041109
[4] Fort J and Pujol T, 2007 *New J. Phys.* **9** 234
[5] Davison K, Dolukhanov P, Sarson G R and Shukurov A, 2006 *J. Archaeol. Sci.* **33** 641
[6] Vlad V O and Ross J, 2002 *Phys. Rev.* E **66** 061908
[7] Fort J, Pérez-Losada J and Isern N, 2007 *Phys. Rev.* E **76** 031913
[8] Méndez V, Ortega-Cejas V and Campos D, 2006 *Physica* A **367** 283
[9] Fort J, Jana D and Humet J, 2004 *Phys. Rev.* E **70** 031913 For the estimation of the generation time $T = 32$ yr, see note [24] in this reference
[10] Fort J and Pujol T, 2008 *Rep. Prog. Phys.* **71** 086001
[11] Merikoski J, Maunuksela J, Myllys M and Timonen J, 2003 *Phys. Rev. Lett.* **90** 024501
[12] Fort J and Méndez V, 2002 *Phys. Rev. Lett.* **89** 178101
[13] Fedotov S and Iomin A, 2007 *Phys. Rev. Lett.* **98** 118101



J. Stat. Mech. (2008) P10012

[14] Fort J and Méndez V, 1999 *Phys. Rev. Lett.* **82** 867
[15] Hamilton M J and Buchanan B, 2007 *Proc. Natl Acad. Sci.* **104** 15625
[16] Fort J, Pérez-Losada J, Suñol J J, Escoda L and Massaneda J M, 2008 *New J. Phys.* **10** 43045
[17] Murray J D, 2002 *Mathematical Biology* 3rd edn, vol 1 (Berlin: Springer)
[18] Méndez V, Campos D and Fort J, 2004 *Europhys. Lett.* **66** 902
[19] Weseloh R M, 2003 *Environ. Entomol.* **32** 111
[20] Kot M, Mark A, Lewis P and van der Driessche P, 1996 *Ecology* **77** 2027
[21] Clark J S, 1998 *Am. Nat.* **152** 204
[22] Birdsell J P, 1957 *Cold Spring Harbor Symp. Quant. Biol.* **22** 47
[23] Roberts D F, 1968 *Nature* **220** 1084
[24] Lotka A J, 1956 *Elements of Mathematical Biology* (New York: Dover) pp 64–9
[25] Fix A G, 1999 *Migration and Colonization in Human Microevolution* (Cambridge: Cambridge University Press)
[26] Stauder J, 1971 *The Majangir. Ecology and Society of a Southwest Ethiopian People* (Cambridge: Cambridge University Press) chapter 10
[27] MacDonald D H and Hewlett B S, 1999 *Curr. Anthropol.* **40** 501
[28] Cavalli-Sforza L L and Bormed W F, 1999 *The Genetics of Human Populations* (New York: Dover) Data for Parma populations is obtained from table 8.7, and for the Issocongos from figure 8.16.B
[29] Ammerman A J and Cavalli-Sforza L L, 1984 *The Neolithic Transition and the Genetics of Population in Europe* (Princeton, NJ: Princeton University Press) chapter 5
[30] Pinhasi R, Fort J and Ammerman A J, 2005 *PLoS Biol.* **3** 2220
[31] Brunet E and Derrida B, 1997 *Phys. Rev.* E **56** 2597
[32] Currat M and Excofier L, 2005 *Proc. R. Soc.* B **272** 679
[33] Harris S, 2003 *Phys. Rev.* E **68** 031912

J. Stat. Mech. (2008) P10012